Model-based fatigue prognosis of fiber-reinforced laminates exhibiting concurrent damage mechanisms

M. Corbetta[1*], C. Sbarufatti[2], M. Giglio[3], A. Saxena[4], K. Goebel[5]

[1,2,3]*Politecnico di Milano, Dipartimento di Meccanica, via La Masa 1, Milan 20156, Italy.*

[4]*General Electric Global Research, 2623 Camino Ramon Suite 500, San Ramon, CA 94583.*

[5]*NASA Ames Research Center, Intelligent Systems Division, MS 269-4, Moffett Field, CA 94035.*

ABSTRACT

Prognostics of large composite structures is a topic of increasing interest in the field of structural health monitoring for aerospace, civil, and mechanical systems. Along with recent advancements in real-time structural health data acquisition and processing for damage detection and characterization, model-based stochastic methods for life prediction are showing promising results in the literature. Among various model-based approaches, particle-filtering algorithms are particularly capable in coping with uncertainties associated with the process. These include uncertainties about information on the damage extent and the inherent uncertainties of the damage propagation process. Some efforts have shown successful applications of particle filtering-based frameworks for predicting the matrix crack evolution and structural stiffness degradation caused by repetitive fatigue loads. Effects of other damage modes such as delamination, however, are not incorporated in these works. It is well established that delamination and matrix cracks not only co-exist in most laminate structures during the fatigue degradation process but also affect each other's progression. Furthermore, delamination significantly alters the stress-state in the laminates and accelerates the material degradation leading to catastrophic failure. Therefore, the work presented herein proposes a particle filtering-based framework for predicting a structure's remaining useful life with consideration of multiple co-existing damage-mechanisms. The framework uses an energy-based model from the composite modeling literature. The multiple damage-mode model has been shown to suitably estimate the energy release rate of cross-ply laminates as affected by matrix cracks and delamination modes. The model is also able to estimate the reduction in stiffness of the damaged laminate. This information is then used in the algorithms for life prediction capabilities. First, a brief summary of the energy-based damage model is provided. Then, the paper describes how the model is embedded within the prognostic framework and how the prognostics performance is assessed using observations from run-to-failure experiments.

Keywords: *CFRP; matrix cracks; delamination; fatigue damage prognosis; particle filtering; sequential Monte Carlo*

1 INTRODUCTION

Recent advancements in real-time structural health monitoring (SHM) methods enable an any-time in-situ assessment of damaged and aging structures' condition and allow collecting data on the progressive, inevitable damage growth due to operating and contingent loads. SHM technologies are increasingly used for fatigue-induced degradation monitoring of composite structures, where the

[1] Post-Doc Associated, matteo.corbetta@polimi.it
[2] Assistant Professor, claudio.sbarufatti@polimi.it
[3] Professor, marco.giglio@polimi.it
[4] Senior Research Scientist, asaxena@ge.com
[5] Tech Area Lead, kai.goebel@nasa.gov

[*] Corresponding author

damage may be hidden in the internal layers and barely visible on the outer surfaces. The availability of information on damage type and damage extent would facilitate also the prediction of the remaining useful life (RUL) of the structure through the estimation of the fatigue damage progression. Addressing the RUL prediction by real-time methods can revolutionize the maintenance policies of aeronautical, mechanical, and civil industry, moving from the current damage tolerance approach to condition-based or predictive maintenance strategies.

However, real-time prediction of RUL of composite materials is a challenging task that must factor in the coexistence of multiple damage mechanisms or multiple damage-modes (MDMs). These damage modes interact with one another and might also generate new damage modes. A typical example is the interaction caused by matrix cracks, delamination and buckling. Matrix cracks can induce local delamination, which can become global delamination, and the delaminated layers can fail because of buckling in case of negative load ratios (i.e., when the minimum load is compressive) [1]. In addition to the coexistence of MDMs, the RUL prediction is inherently affected by several sources of uncertainty. Fatigue of materials is uncertain in nature, since it is driven by inclusions and impurities caused by the manufacturing process and complex physical nano- and micro-scale phenomena not accounted for in common engineering models. Where damage is measured using automated SHM tools, there are additional uncertainties about current damage location and extent that further complicate the prediction of the damage growth. This makes stochastic approaches a logical choice for real-time RUL prediction.

While highly desirable, real-time damage prognosis of composite laminates has so far been only sparsely explored. It requires a methodology to predict the damage evolution that merges stochastic approaches and real-time diagnostic information in the prognostic stage to update the RUL prediction. Recently, Bayesian filters have shown promising results in predicting the evolution of matrix cracks and consequent stiffness degradation of cross-ply laminates by including SHM data in the prognostic stage [2]. However, the effect of co-existing damage mechanisms was not incorporated in the damage progression model, and the resulting stiffness degradation was only linked to the presence of matrix cracks.

The work reported herein follows the methodology proposed in [2] and extends the Bayesian framework by including an energy-based MDM model. This model was recently investigated in [3], where the authors showed successful predictions of the stiffness degradation caused by matrix cracks and delamination in cross-ply fiber-reinforced laminates. Here, the MDM model is embedded in a Bayesian filtering algorithm commonly referred to as *particle filtering* [4], which aims at simultaneously monitoring three degradation processes: matrix crack density, delamination and stiffness reduction. The energy-based MDM model enables the estimation of the interacting damage growth rates, and the embedding of the mechanical model into the Bayesian framework allows the probabilistic estimation of the RUL conditioned upon the available diagnostic data. The developed model-based prognostic framework is assessed against tension-tension fatigue damage progression data on a carbon fiber-reinforced polymer (CFRP) laminate. The growing damages were observed through X-ray images and quantified dimensions are provided to the algorithm sequentially, thus simulating a real-time condition where a SHM system provides regular information on the damage extent as time passes by.

The rest of the paper organizes as follows: Section 2 introduces the MDM model and the equations to predict the damage progression, Section 3 shows the probabilistic framework based on particle filtering and the basic probability density functions (PDFs) to implement the algorithm and Section 4 shows the application on CFRP damage growth data. Section 5 draws some conclusions.

2 MODELING OF CONCURRENT DAMAGE PROGRESSION

Most of the models for damage growth prediction in composites resort on finite element methods because of the complexity of the damage mechanisms and their interactions. However, the computational costs of finite element methods prevent the applicability of resulting models in stochastic algorithms for real-time applications. Analytical damage progression models are,

therefore, preferred in real-time prognostic scenarios: where the model complexity can be scaled down to perform a fast estimation of the damage progression using simplified formulations of the stress state [3]. In addition, the tuning of analytical models is usually easier because of the limited number of model parameters.

The approach proposed here, which follows [2], uses a *strain energy release rate* (SERR) model, since the stress intensity factor-based models, otherwise widely adopted in metal fatigue, lose their usefulness when several cracks and different damage mechanisms affect the material. The formulation of the SERR includes the effect of matrix cracks and delamination, $G = G(\rho, D)$, which are the two most common damage mechanisms affecting fiber-reinforced laminates [5]. The model also provides an estimation of the Young's modulus of the damaged laminate E_x, thereby enabling the monitoring of the stiffness degradation.

The SERR range ΔG, caused by fatigue loads, is used as an input to power law models for the estimation of the damage growth rates, expressed as damage growth per load cycle [6]. These power laws are commonly named *modified Paris' laws*, given the similarity to Paris' law used for metallic alloys. The growth rates of matrix crack density ρ and delamination D are, therefore, expressed using:

$$\frac{\mathrm{d}\rho}{\mathrm{d}N} = A\big(\Delta G(\rho, D)\big)^{\alpha}, \tag{1}$$

$$\frac{\mathrm{d}D}{\mathrm{d}N} = B\big(\Delta G(\rho, D)\big)^{\beta}. \tag{2}$$

The closed form solution of (1) and (2) rarely exists, since G is understood to be a highly nonlinear function of the damage severity. So, the alternative is the estimation of the damage progression using a linear damage accumulation rule:

$$\rho_k = \rho_{k-1} + \left.\frac{\mathrm{d}\rho}{\mathrm{d}N}\right|_{\rho_{k-1}, D_{k-1}} \Delta N, \tag{3}$$

$$D_k = D_{k-1} + \left.\frac{\mathrm{d}D}{\mathrm{d}N}\right|_{\rho_{k-1}, D_{k-1}} \Delta N, \tag{4}$$

where ΔN is the number of load cycles between two discrete time-steps, *k-1* and *k*. Since G for composite laminates is particularly high during the first stage of the fatigue life, large time steps (i.e., large ΔN) can generate inaccurate solutions. Therefore, ΔN is usually kept equal to 1 to simulate the damage growth correctly. Once the amount of damage has been calculated, the ratio of the current elastic modulus E_x (depending on ρ and D) and the initial elastic modulus $E_{x,0}$ determines the normalized remaining stiffness of the laminate:

$$S = \frac{E_x(\rho, D)}{E_{x,0}}. \tag{5}$$

The work in [3] investigated the capability of both matrix crack-induced delamination models and edge delamination models in describing the SERR as a function of matrix cracks and delamination and in estimating the laminate remaining stiffness as well. The study pointed out as the edge delamination model proposed by Zhang, Soutis and Fan [7] appeared as the best in describing the stiffness reduction of a notched cross-ply laminate already utilized in [2]. Zhang et al. analyzed the pioneering work of O'Brien [8], introducing the effective elastic modulus of a partially-delaminated laminate, and they enhanced this model including the effect of matrix cracks in the laminated region.

The model requires some simplifying assumptions on the type and shape of delamination, crack pattern and crack location. Specifically, this model was developed for symmetric balanced laminates under tensile loading and matrix cracks spanning full width of the 90° plies. Fig. 1 shows a graphical representation of the model, using a $[0_n/90_m]_s$ stacking sequence. Delamination D is assumed to full length of the laminate (x-direction) and grows along the width, transverse to the applied load (y-direction); it is expressed in meters, m. The matrix crack density ρ is measured as number of cracks per unit length, #/m.

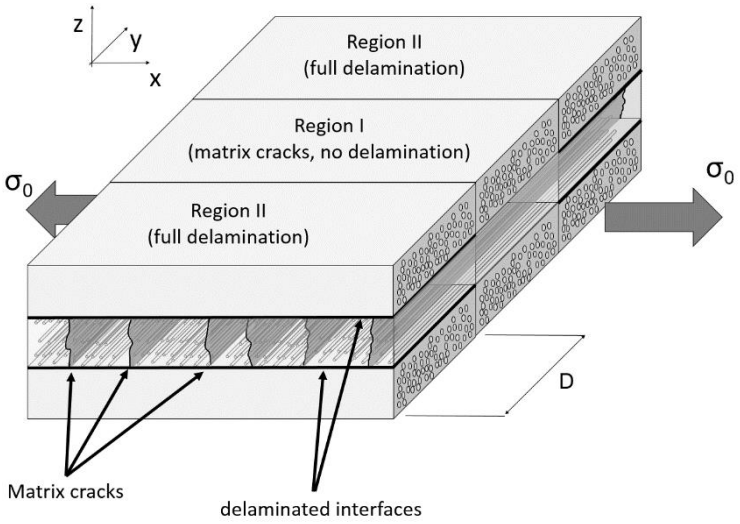

Figure 1. Zhang's model for a partially-delaminated cross-ply laminate [7].

In this case, the outer sub-laminates are aligned with the direction of the remote tensile stress σ_0 indicated by the thick arrows (0° sub-laminates). The inner sub-laminate is perpendicular to the load direction (90° sub-laminate) and is affected by fatigue-induced matrix cracks. This configuration splits the laminate in three regions, two of which are symmetric. Therefore, only two distinct regions are created based on different features. Region I is the laminated region where delamination is absent and the matrix cracks in the 90° plies reduce the sub-laminate stiffness. Region II represents the fully-delaminated region where the 0° sub-laminates are assumed to have disconnected from the 90° sub-laminate. The two regions have different longitudinal elastic moduli named $E_{x,I}$ and $E_{x,II}$, respectively. The effective elastic modulus of the laminate is calculated as the weighted average of the two elastic moduli,

$$E_x(\rho, D) = E_{x,I}(\rho) + \left[E_{x,II} - E_{x,I}(\rho)\right]\frac{D}{W}, \tag{6}$$

where $E_{x,II}$ depends on the number of delaminated interfaces. If both the interfaces between the 0° and 90° sub-laminates are delaminated (as shown in Fig. 1), $E_{x,II}$ can be easily calculated using the laminate theory [1]. The matrix crack density ρ influences $E_{x,I}$, as modeled in [7] by means of *in-situ damage effective functions* (IDEFs), $\Lambda = \Lambda(\rho)$, which affects the stiffness matrix Q of the 90° plies:

$$Q(\rho) = \begin{bmatrix} Q_{11,0} & Q_{12,0} & 0 \\ Q_{21,0} & Q_{22,0} & 0 \\ 0 & 0 & Q_{66,0} \end{bmatrix} - \begin{bmatrix} Q_{12,0}^2/Q_{22,0} & Q_{12,0} & 0 \\ Q_{21,0} & Q_{22,0} & 0 \\ 0 & 0 & Q_{66,0} \end{bmatrix} \begin{bmatrix} \Lambda_{22}(\rho) \\ \Lambda_{22}(\rho) \\ \Lambda_{66}(\rho) \end{bmatrix}. \tag{7}$$

The IDEFs $\Lambda_{22}(\rho)$ and $\Lambda_{66}(\rho)$ were determined by Zhang and coauthors in previous works [9]. They are based on a modified two-dimensional shear lag analysis and they describe the in-situ constraint conditions of the 90° plies. The equations to derive the IDEFs are not reported here for the sake of brevity. Interested reader is referred to the original papers [7]-[9] for more details. Eventually, the SERR is calculated using:

$$G(\rho, D) = \varepsilon(\rho, D)^2 \frac{h}{n_d}\left(E_{x,I}(\rho) - E_{x,II}\right), \tag{8}$$

where $\varepsilon(\rho, D) = \sigma_0/E_x\,(\rho, D)$ and any thermal effect has been neglected. As explained above, the SERR G is embedded into the damage growth rate and the longitudinal elastic modulus of the damaged laminate $E_x(\rho, D)$ is used to estimate the remaining stiffness. It is worth noting that the SERR range ΔG has been defined by:

$$\Delta G = \left(\sqrt{G_{max}} - \sqrt{G_{min}}\right)^2, \tag{9}$$

$$\begin{aligned} G_{max} &= G(\sigma_{0,max}) \\ G_{min} &= G(\sigma_{0,min}) \end{aligned}. \tag{10}$$

In this way, the mean load effect, which can alter the similitude criterion, is neglected [10]. The SERR range in (9) is inserted in Eqq. (1) and (2) to calculate the damage growth rates, and the model used in particle filtering is then composed by Eqq. (3)-(5).

3 PARTICLE FILTERING-BASED PROGNOSIS

This section describes the prognostic framework that composes of the MDM model in Section 2 and particle filtering. Specifically, a *bootstrap* sequential importance resampling algorithm with systematic resampling has been chosen to build the Bayesian framework [11]. Furthermore, a sub-algorithm has been used to update the model parameter during run-time. The fundamental equations used in the algorithm are summarized and directly tailored for the fatigue damage prognosis problem below.

Let us consider the system's state $\boldsymbol{x}$ governed by a dynamic state-space (DSS) model:

$$\begin{aligned} \boldsymbol{x}_k &= f(\boldsymbol{x}_{k-1}, \boldsymbol{\theta}, \boldsymbol{u}_{k-1}, \boldsymbol{\omega}_{k-1}) \\ \boldsymbol{z}_k &= g(\boldsymbol{x}_k, \boldsymbol{\eta}_k) \end{aligned}. \tag{11}$$

The system's state vector contains the three damage modes $\boldsymbol{x}_k = [\rho_k, D_k, S_k]^T$, while the measurement vector contains the observations of the true (unknown) system's state $\boldsymbol{z}_k = \left[\hat{\rho}_k, \widehat{D}_k, \hat{S}_k\right]^T$. The evolution equation f describes the system's state dynamics and is driven by Eqq. (3)-(5). Instead, the observation equation g links the measures with the damage state. The uncertainties affecting the system's state dynamics and the measurement system are embedded in the DSS model using random processes called process noise $\boldsymbol{\omega}_k$, and measurement noise $\boldsymbol{\eta}_k$, respectively. Since both the system's state vector and the measurement vector are three-dimensional, the noise terms have been split in three independent expressions. Following the discussion in [12], the errors affecting the matrix crack density and delamination models are defined as log-Normal random processes e^{ω}, while the error of the stiffness degradation model is an unbiased Gaussian random process:

$$\boldsymbol{x}_k = \begin{bmatrix} \rho_k \\ D_k \\ S_k \end{bmatrix} = \begin{bmatrix} \rho_{k-1} + \frac{d\rho}{dN}(\boldsymbol{\theta}, \boldsymbol{u}_{k-1})\Big|_{\rho_{k-1}, D_{k-1}} e^{\omega_\rho} \\ D_{k-1} + \frac{dD}{dN}(\boldsymbol{\theta}, \boldsymbol{u}_{k-1})\Big|_{\rho_{k-1}, D_{k-1}} e^{\omega_D} \\ \frac{E_x(\rho_k, D_k)}{E_{x,0}} + \omega_S \end{bmatrix}. \tag{12}$$

The measurement noise terms are modeled as independent, unbiased Gaussian processes:

$$\boldsymbol{z}_k = \begin{bmatrix} \hat{\rho}_k \\ \widehat{D}_k \\ \hat{S}_k \end{bmatrix} = \begin{bmatrix} \rho_k + \eta_\rho \\ D_k + \eta_D \\ S_k + \eta_S \end{bmatrix}. \tag{13}$$

Equation (12) shows the dependence of the damage growth rates on the model parameter vector $\boldsymbol{\theta}$ and the input vector $\boldsymbol{u}$. The latter is the far-field stress range that drives ΔG, so $\boldsymbol{u} \rightarrow u = \Delta\sigma_0 = \sigma_{max} - \sigma_{min}$. As already presented in [12], the use of a log-Normal random process with specific relation between mean and variance produces an unbiased evolution equation. The process noise $\boldsymbol{\omega}$ follows:

$$\begin{aligned} \boldsymbol{\omega} &= \left[\omega_\rho, \omega_D, \omega_S\right] \sim MVN(\mu_\omega, \Sigma_\omega) \\ \mu_\omega &= \left[-\frac{\sigma_{\omega,\rho}^2}{2}, -\frac{\sigma_{\omega,D}^2}{2}, 0\right]^T \\ \Sigma_\omega &= \begin{bmatrix} \sigma_{\omega,\rho}^2 & 0 & 0 \\ 0 & \sigma_{\omega,D}^2 & 0 \\ 0 & 0 & \sigma_{\omega,S}^2 \end{bmatrix} \end{aligned}, \tag{14}$$

while the measurement noise is unbiased Gaussian $\boldsymbol{\eta} \sim MVN\left(0, \Sigma_\eta\right)$. The process and measurement noise terms have been modeled as stationary random processes; therefore, their dependence from the time step *k* has been neglected. The model parameter vector $\boldsymbol{\theta}$ can be updated during run time to improve the prediction performance of the algorithm. Here, the *artificial dynamics* sub-algorithm has been used for its simplicity and effectiveness [13]. It introduces a perturbation of the model parameter values using a random disturbance $\boldsymbol{\gamma}$, usually defined as an unbiased Gaussian process:

$$\boldsymbol{\theta}_k = \boldsymbol{\theta}_{k-1} + \boldsymbol{\gamma}_{k-1}, \tag{15}$$

where $\boldsymbol{\gamma}_k \sim \mathcal{N}\left(0, \Sigma_{\boldsymbol{\gamma},k}\right)$. The covariance matrix $\Sigma_{\boldsymbol{\gamma},k}$ must decrease as time passes by to guarantee the convergence of the algorithm [13]. In this application, the covariance function has been chosen empirically according to the authors' experience and follows

$$\Sigma_{\boldsymbol{\gamma},k} = \frac{1}{2k}\Sigma_{\boldsymbol{\gamma},0}, \tag{16}$$

where $\Sigma_{\boldsymbol{\gamma},0}$ is the initial covariance matrix and *k* is the time step. The model parameter vector contains the empirical parameters of the modified Paris' laws in Eqq. (1) and (2), $\boldsymbol{\theta} = [\log A\,, \alpha, \log B\,, \beta]^T$. The two parameters *A* and *B* have been embedded using their logarithmic form, since they are log-Normally distributed [14].

The sequential importance resampling method allows the approximation of the conditional PDF of the system's state and model parameter given the observations, $p(\boldsymbol{x}_k, \boldsymbol{\theta}_k | \boldsymbol{z}_{0:k})$, using N_s weighted samples:

$$p(\boldsymbol{x}_k, \boldsymbol{\theta}_k | \boldsymbol{z}_{0:k}) \approx \sum_{i=1}^{N_s} w_k^{(i)} \delta\left(\boldsymbol{x}_k^{(i)} - \boldsymbol{x}_k\right)\left(\boldsymbol{\theta}_k^{(i)} - \boldsymbol{\theta}_k\right), \tag{17}$$

where the pairs $\left\{\boldsymbol{x}_k^{(i)}, \boldsymbol{\theta}_k^{(i)}\right\}_{i=1}^{N_s}$ are Monte Carlo samples of the system's state and model parameters, which are weighted by the weights $w_k^{(i)}, i = 1, \ldots, N_s$. Following the *bootstrap particle filtering* theory, the samples $\boldsymbol{x}_k^{(i)}$ and $\boldsymbol{\theta}_k^{(i)}$ are generated through the evolution equation and the artificial dynamics equation:

$$\begin{aligned} \boldsymbol{x}_k^{(i)} &= f\left(\boldsymbol{x}_{k-1}^{(i)}, \boldsymbol{\theta}_{k-1}^{(i)}, \boldsymbol{u}_{k-1}, \boldsymbol{\omega}^{(i)}\right) \\ \boldsymbol{\theta}_k^{(i)} &= \boldsymbol{\theta}_{k-1}^{(i)} + \boldsymbol{\gamma}_{k-1}^{(i)} \end{aligned}, \tag{18}$$

where $\boldsymbol{\gamma}_{k-1}^{(i)}$ is a sample from $\mathcal{N}\left(0, \Sigma_{\boldsymbol{\gamma},k}\right)$ and $\boldsymbol{\omega}^{(i)}$ is a sample from $MVN(\mu_\omega, \Sigma_\omega)$. It should be noted that the subscript *k* on the model parameter vector refers to the fact that the samples are from the *k-th* posterior estimation, because the true $\boldsymbol{\theta}$ is not time-varying. The weights $w_k^{(i)}$ depend on the likelihood of the observation given the sample $p\left(\boldsymbol{z}_k | \boldsymbol{x}_k^{(i)}\right)$, and are then normalized to sum up to 1,

$$\begin{aligned} \widetilde{w}_k^{(i)} &= w_{k-1}^{(i)} p\left(\boldsymbol{z}_k | \boldsymbol{x}_k^{(i)}\right) \\ w_k^{(i)} &= \frac{\widetilde{w}_k^{(i)}}{\sum_{j=1}^{N_s} \widetilde{w}_k^{(i)}} \end{aligned}. \tag{19}$$

The prediction step is carried out by propagating the samples of the system's state in the future using the evolution equation $f(\cdot)$. At each time step, the system's state sample $\boldsymbol{x}^{(i)}$ is altered by a sample of the model error $\boldsymbol{\omega}^{(i)}$, which simulates the unpredictable fluctuations of the damage growth rates caused by small-scale phenomena, otherwise, neglected in the model. The prognosis is analytically expressed through the *p-step ahead prediction equation* ([15]):

$$\hat{p}(\boldsymbol{x}_{k+p}|\boldsymbol{z}_{0:k}) = \sum_{i=1}^{N_s} w_k^{(i)} \int_{\mathcal{D}} p\left(\boldsymbol{x}_{k+1}|\boldsymbol{x}_k^{(i)}\right) \prod_{j=k+2}^{k+p} p(\boldsymbol{x}_j|\boldsymbol{x}_{j-1}) d\boldsymbol{x}_{k+1:k+p-1}, \tag{20}$$

where $p(\boldsymbol{x}_j|\boldsymbol{x}_{j-1})$ is the *transition density function*, which comes from the probabilistic form of the evolution equation $f(\cdot)$. Once the posterior distribution of the system's state has been computed, the samples $x_k^{(i)}$ are projected into the future using the transition density function (i.e., the evolution equation). The concept behind the prediction equation (Eq. (20)) can be further extended to calculate the number of fatigue load cycles to reach a pre-determined critical threshold, $\boldsymbol{x}_{CR}$. The samples of the system's state are propagated until they reach the threshold, i.e., $\boldsymbol{x}_{k+l}^{(i)} = \boldsymbol{x}_{CR}$. The number of fatigue load cycles corresponding to the time step $k + l$ is defined as the end of life of the sample, $N_f^{(i)}$. Thus, the RUL of the *i-th* sample is the difference between $N_f^{(i)}$ and the number of load cycles of the current time step, $\mathrm{RUL}_k^{(i)} = N_f^{(i)} - N_k$. Once all the samples have crossed the critical threshold, the sample pairs $\left\{\mathrm{RUL}_k^{(i)}, w_k^{(i)}\right\}_{i=1}^{N_s}$ are used to estimate the RUL distribution as follows:

$$p(\mathrm{RUL}_k|\boldsymbol{z}_{0:k}) \approx \sum_{i=1}^{N_s} w_k^{(i)} \delta\left(\mathrm{RUL}_k^{(i)} - \mathrm{RUL}_k\right). \tag{21}$$

Here, the critical threshold has been defined as a limit damage state $\boldsymbol{x}_{CR} = [\rho_{CR}, D_{CR}, S_{CR}]^T$ that should not be crossed to guarantee the safety of the structure. Once the *i-th* sample $\boldsymbol{x}_k^{(i)}$ reaches one of the limits (either ρ_{CR}, D_{CR} or S_{CR}), the sample's propagation stops and the related $\mathrm{RUL}_k^{(i)}$ is recorded to compute the RUL distribution.

4 APPLICATION TO REAL FATIGUE-INDUCED DAMAGES IN CFRP LAMINATES

The algorithm in Section 3 is applied to fatigue damage progression data publicly available from the NASA prognostics data repository [16]. These data refer to fatigue experiments on the notched cross-ply coupon *L1S11* with dog-bone geometry and stacking sequence $[0_2/90_4]_s$. Details on the tension-tension fatigue tests are available in [17]. The data acquisition stopped on a maximum of $N_f = 100\,000$ load cycles applied through a load frequency of 5 Hz, sinusoidal shape, maximum force $F = 31$ kN and load ratio $R \approx 0.14$. The outer coupon dimensions are 152.4 mm × 254 mm [width × height], and the material properties of the Torayca T700G plies are expressed in *Table 1*.

Table 1. Ply properties

Young's modulus	E_1	[GPa]	127.55
Transverse elastic modulus	E_2	[GPa]	8.41
In-plane Poisson's ratio	ν_{12}	[-]	0.309
In-plane shear modulus	G_{12}	[GPa]	6.2
Out-of-plane shear modulus	G_{23}	[GPa]	2.82
Thickness	t	[mm]	0.152

A series of X-ray images frequently collected during the test allowed the quantification of the internal damage (matrix crack density and delamination), and a tri-axial strain gauge rosette on the outer surface was used to record the strains, Fig. 2.

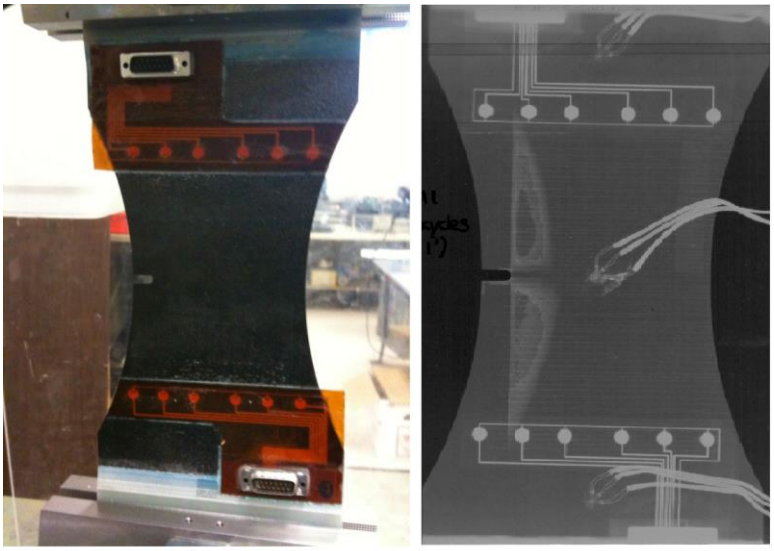

(a) (b)

Figure 2. Notched cross-ply coupon under test (a), and X-ray image (b). The light gray region close to the notch is the delaminated region, while the horizontal, light gray lines are the matrix cracks that span the width of the 90° sub-laminate.

X-ray images were processed to quantify matrix crack density, delamination, and strain-gauge data were used to estimate the reduction in stiffness. The work in [3] summarizes the procedure to extract the amount of damage from the X-rays. Given the first damage assessment, the algorithm provides an estimation of the RUL, which is systematically updated whenever a new measurement becomes available. The number of samples used for running the algorithm is $N_s = 15000$. The initialization values of the noise variances and the model parameter vector used are reported in *Table 2*. The model parameters have been initialized using estimates based on other coupons. The critical threshold is set equal to the amount of damage observed at $N_f = 100\,000$ load cycles, which is $\boldsymbol{x}_{CR} = [\rho_{CR},\ D_{CR},\ S_{CR}]^T = [422,\ 0.0229,\ 0.88]^T$.

Table 2. Initialization of random noise and model parameter vector

	$\boldsymbol{\omega}$			$\boldsymbol{\eta}$			$\boldsymbol{\theta}$			
	ω_ρ	ω_D	ω_S	η_ρ	η_D	η_S	$\log A$	α	$\log B$	β
	[-]	[-]	[-]	[#/m]	[m]	[-]	$\left[\frac{\#/m}{(J/m^2)^\beta}\right]$	[-]	$\left[\frac{m}{(J/m^2)^\beta}\right]$	[-]
μ	-5	$-0.5\cdot10^{-3}$	0	0	0	0	-11.5	3.3	-21.9	3.5
σ^2	10	$1\cdot10^{-3}$	$5\cdot10^{-6}$	80	$1\cdot10^{-6}$	$7\cdot10^{-5}$	0.85	0.01	0.85	0.01

The filtered estimate of the damage progression is shown in Fig. 3. Every time a new observation becomes available, the updating of the weights $w_k^{(i)}$ consents to estimate the posterior distribution of the system's state. The expected values and the confidence bands of the filtered estimates are representative of the goodness of the algorithm in monitoring the multiple, concurrent damage mechanisms. The matrix crack density estimation seems to be well captured by the algorithm; the expected value approaches the observed matrix crack density as time passes by. Delamination, however, is slightly underestimated by the algorithm for most of the fatigue life, while the estimated trend of the normalized stiffness has very narrow confidence bands, insomuch as most of the experimental observations fall outside the 99% of the σ-band. Though, the observations of the stiffness degradation appear noisy, and the estimated trend seems to fall in between the observations. Then, the algorithm seems to be able to filter out disturbances and concentrates the samples in between the noisy observations correctly.

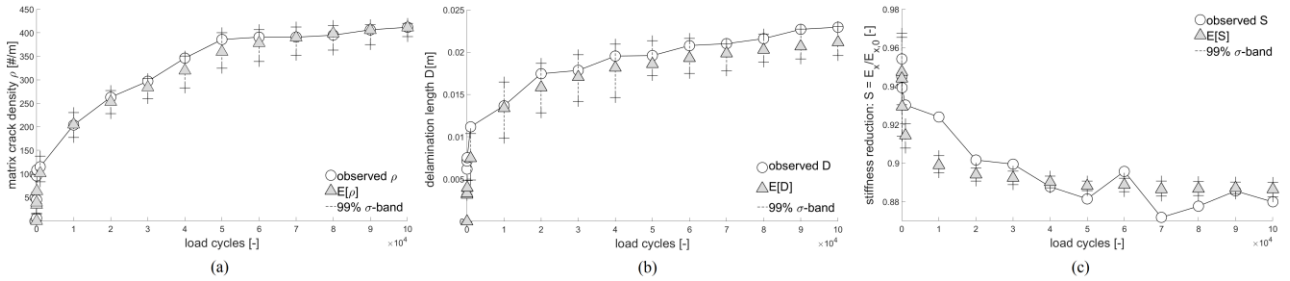

Figure 3. Posterior estimation of the damage growth against load cycles; matrix crack density (a), delamination (b) and normalized stiffness (c).

After every posterior estimation of the damage state, the samples are further projected into the future using the prediction equation (Eq. (20)) to predict the RUL. The performance of sequential estimation of the RUL is reported in Fig. 4. The RUL prediction is already close to the true RUL since the very beginning of the fatigue life, after only a few load cycles. Though, the wide confidence band of the prediction suggests that the information is characterized by large uncertainty. Then, the confidence band shrinks over time, but the average RUL moves away from the true value (between 10 000 and 40 000 load cycles). This implies that the values of the model parameters are changing during this stage to better fit the available data. After N = 50 000 load cycles, the expected RUL converges close to the correct value. The confidence band also keeps shrinking around the average RUL, thus indicating improvement in prediction performance with time.

5 CONCLUSION

This work proposes a model-based Bayesian framework for composite laminates exhibiting concurrent damage mechanisms. An energy-based model that is able to estimate the SERR and the longitudinal elastic modulus constitutes the core of the fatigue damage accumulation model, and the latter is embedded into a Bayesian framework of particle filtering. The approach has been already presented in the recent literature for monitoring the growth of matrix crack density, but the algorithm proposed here enables the real-time monitoring and prediction of coexisting damage modes, which interact with one another and their combined effect influences the remaining life of the structure. The methodology has been successfully applied to CFRP damage progression data obtained through tension-tension fatigue experiments.

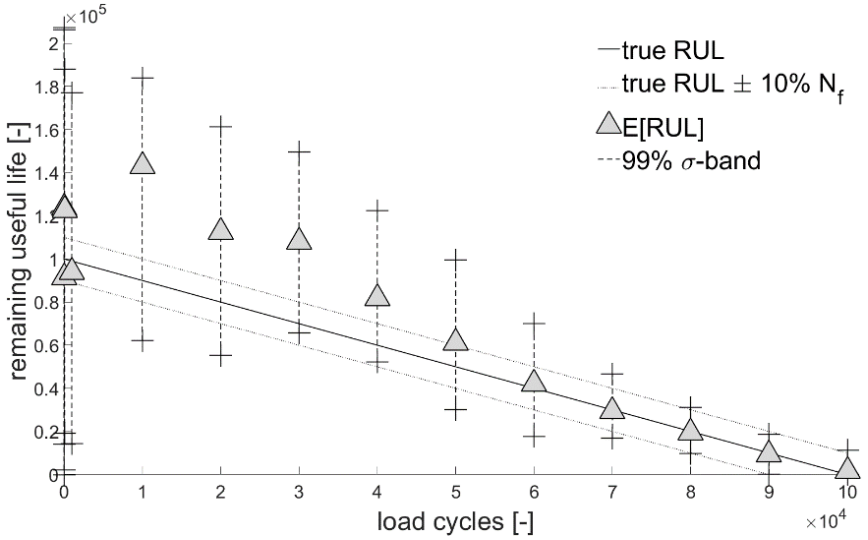

Figure 4. RUL prediction. The two additional lines indicating the band RUL ± 10% of the end of life help in evaluating the goodness of the prediction.

The filtered estimation of the damage extent shows that the algorithm slightly underestimates the observed delamination growth. The posterior expectation of the matrix crack density is in line with the observed ρ, and the estimated stiffness degradation appears well-centered on the noisy observations made with the strain gauge. Large fluctuations in the RUL predictions characterize the early-mid stage of the fatigue life, but the expected value successfully converges to the true RUL after 50 000 load cycles and remains close to the target RUL until the end of the test.

Future research should include the application of the prognostic method to other fatigue damage progression data. This is an important step to verify algorithm performance and generalize the validity of the approach. The number of samples N_s has been chosen with a trial & error approach, and it is likely not the overall best choice to explore the state-space correctly. The use of refined methods to select N_s can improve the algorithm performance and save computational time. In line with this idea, real-time, non-parametric methods to select (or update) the variance of the artificial dynamics perturbation can enhance the model parameter updating. Also, the use of refined sub-algorithms for the real-time parameter updating, like the *kernel smoothing* method may speed-up the convergence of the RUL prediction. Eventually, the definition of the end-of-life of CFRPs according to the asymptotic damage behavior should be further investigated. As a matter of fact, the horizontal asymptote representing the critical damage state can significantly change with the coupon because of the natural, inherent variability of the material. Therefore, a general and unified guideline to define the RUL of a composite laminate would be valuable.

NOMENCLATURE

A	modified Paris' law parameter
B	modified Paris' law parameter
D	transverse delamination
E_x	longitudinal elastic modulus
G	strain energy release rate
N	load cycle
N_f	end-of-life (in cycles)
N_s	number of samples
Q	stiffness matrix of the 90° plies
$Q_{ij,0}$	stiffness element of the undamaged ply in the *i*-*j* direction
S	normalized stiffness
W	laminate half-width
f	evolution equation
g	observation equation
h	laminate half-thickness
k	time step
n_d	number of delaminated interfaces
u	input
w	sample weight
x	system state
z	observation
Λ	in-situ damage effective function
α	modified Paris' law parameter
β	modified Paris' law parameter
γ	Gaussian random process
δ	Kronecker delta
ε	far-filed strain
η	measurement noise

θ model parameter
ρ matrix crack density
σ_0 far-field stress
ω process noise

ACKNOWLEDGEMENT

Part of the material of this paper is based upon work supported by NASA under award No: NNX12-AK33A. The first author would like to thank the Structures and Composites Laboratory (SACL) at Stanford University for the data on the matrix crack density, the Prognostics Center of Excellence at NASA Ames Research Center, and the University Space Research Association (USRA).

REFERENCES

[1]. Talreja, R. & Singh, C. V. *Damage and failure of composite materials*. Cambridge University Press, 2012.
[2]. Chiachio, M., Chiachio, J., Saxena, A., Rus, G. & Goebel, K. Fatigue damage prognosis in FRP composites by combining multi-scale degradation fault modes in an uncertainty Bayesian framework. *Proceedings of Structural Health Monitoring*, 2013; **1**.
[3]. Corbetta, M., Saxena, A., Giglio, M. & Goebel, K. Evaluation of multiple damage-mode models for prognostics of carbon fiber-reinforced polymers. *10th International Workshop on structural Health Monitoring: System Reliability for Verification and Implementation*, 2015; **2**:609-616.
[4]. Gordon, N. J., Salmond, D. J. & Smith, A. F. Novel approach to nonlinear/non-Gaussian Bayesian state estimation. *IEEE Proceedings F (Radar and Signal Processing)*, 1993; **140**:107-113.
[5]. Nairn, J. A. Matrix Microcracking in Composites, in *Polymer Matrix Composites*, Chapter 13, R. Talreja and J-A Manson, Volume 2 of *Comprehensive Composite Materials*, A. Kelly and C. Zweben, 2000, Elsevier Science.
[6]. Degrieck, J. & Van Paepegem, W. Fatigue damage modeling of fibre-reinforced composite materials: Review. *Applied Mechanics Reviews, American Society of Mechanical Engineers*, 2001; **54**:279-300.
[7]. Zhang, J., Soutis, C. & Fan, J. Effects of matrix cracking and hygrothermal stresses on the strain energy release rate for edge delamination in composite laminates. *Composites* 1994; **25**:27-35.
[8]. O'Brien, T. Characterization of delamination onset and growth in a composite laminate Damage in composite materials, *American Society for Testing and Materials, ASTM STP*, 1982; **775**:140-167.
[9]. Zhang, J., Fan, J. & Soutis, C. Analysis of multiple matrix cracking in $[\pm\theta_m/90_n]_s$ composite laminates. Part 1: In-plane stiffness properties. *Composites* 1992; **23(5)**:291-298.
[10]. Rans, C., Alderliesten, R. & Benedictus, R. Misinterpreting the results: how similitude can improve our understanding of fatigue delamination growth. *Composites Science and Technology* 2011; **71**:230-238.
[11]. Arulampalam, M. S., Maskell, S., Gordon, N. & Clapp, T. A tutorial on particle filters for online nonlinear/non-Gaussian Bayesian tracking. *Signal Processing, IEEE Transactions on* 2002; **50**:174-188.
[12]. Corbetta, M., Sbarufatti, S. & Giglio, M. Optimal tuning of particle filtering random noise for monotonic degradation processes. *Proceedings of the third European Conference of the Prognostics and Health Management Society*, Bilbao, Spain, 2016.
[13]. Liu, J. & West, M. Combined parameter and state estimation in simulation-based filtering. In *Sequential Monte Carlo methods in practice*, Springer, 2001; 197-223.
[14]. Corbetta, M., Sbarufatti, C., Manes, A. & Giglio, M. On dynamic state-space models for fatigue-induced structural degradation, *International Journal of Fatigue* 2014; **61**:202-219.
[15]. Doucet, A., Godsill, S. & Andrieu, C. *On sequential Monte Carlo sampling methods for Bayesian filtering*. Statistics and computing, Springer, 2000; **10**:197-208.
[16]. Saxena, A., Goebel, K., Larrosa, C. & Chang, F.-K. *CFRP composites dataset*. NASA Ames prognostics data repository, 2008.
[17]. Saxena, A., Goebel, K., Larrosa, C., Janapati, V., Roy, S. & Chang, F.-K. *Accelerated aging experiments for prognostics of damage growth in composite materials*. DTIC Document, 2011.